CSIRO PUBLISHING

International Journal of Wildland Fire **2009**, *18*, 404–414 www.publish.csiro.au/journals/ijwf

Integration of AWiFS and MODIS active fire data for burn mapping at regional level using the Burned Area Synergic Algorithm (BASA)

Federico González-Alonso[A] *and Silvia Merino-de-Miguel*[B,C]

[A]Remote Sensing Laboratory, Centro de Investigación Forestal – Instituto Nacional de Investigación y Tecnología Agraria y Alimentaria (CIFOR-INIA), Ctra. A Coruña, km 7.5, E-28040 Madrid, Spain.

[B]Escuela Universitaria de Ingeniería Técnica Forestal (EUIT Forestal), Universidad Politécnica de Madrid, Ciudad Universitaria, s/n, E-28040 Madrid, Spain.

[C]Corresponding author. Email: silvia.merino@upm.es

Abstract. The present paper presents an algorithm that synergistically combines data from four different parts of the spectrum (near-, shortwave, middle- and thermal infrared) to produce a reliable burned-area map. It is based on the use of a modified version of the BAIM (MODIS – Moderate Resolution Imaging Spectrometer – Burned Area Index) together with active fire information. The following study focusses in particular on an image from the AWiFS (Advanced Wide Field Sensor) sensor dated 21 August 2006 and MODIS active fires detected during the first 20 days of August as well as ancillary maps and information. The methodology was tested in Galicia (north-west Spain) where hundreds of forest fires occurred during the first 20 days of August 2006. Burned area data collected from the present work was compared with official fire statistics from both the Spanish Ministry of the Environment and the Galician Forestry Service. The speed, accuracy and cost-effectiveness of this method suggest that it would be of great interest for use at both regional and national levels.

Additional keywords: BAIM, forest fires, Mediterranean basin, remote sensing.

Introduction

Forest fires are a major source of concern not only for environmental reasons, but also those including economy, society and human safety in many parts of the world, including the Mediterranean countries of southern Europe. This particular geographical area is characterised by high temperatures and low rainfall during the summer months, which, together with an increased accumulation of forest fuels due to the abandonment of rural areas, is causing the area that is prone to wildfires to grow (Chuvieco 1999). Moreover, forest fires play an important role in global climate change, being responsible for the release of a significant amount of greenhouse gases, particulates and aerosol emissions into the atmosphere (Crutzen and Andreae 1990). Houghton *et al*. (1995) state that biomass burning contributes up to 40% of the total emissions of anthropogenic origin of CO_2. According to Van der Werf *et al*. (2006), forest fires emitted 8406×10^6 t of CO_2 during 2004, a figure that accounts for 32% of the CO_2 emissions for all developed countries in that year (United Nations Framework Convention on Climate Change, http://unfccc.int, accessed 18 March 2009).

The use of traditional methods to map and quantify these events is expensive and time-consuming (González-Alonso *et al.* 2007), so remote sensing observation's ability to supply 'a suitable alternative to conventional techniques for mapping the extent of burned areas, as well as for providing post-fire related information' (Mitri and Gitas 2006) is an effective alternative. Remote sensing estimations of burned areas are quick, reliable and cost-effective, factors that, in turn, facilitate the establishment of rapid response systems. Additionally, maps produced using remote sensing could be combined with slope and soil type maps, in order to locate priority intervention areas and plan forest restoration work (Roldán-Zamarrón *et al.* 2006).

The assessment of burned areas at a regional to global scale is presently only affordable using remote sensing techniques, as demonstrated by initiatives like the Global Burnt Area 2000 (GBA2000), the GLOBSCAR, the GLOBCARBON Burnt Area Estimate (BAE) Product or the MODIS (Moderate Resolution Imaging Spectrometer) Burned Area Product. The GBA2000 initiative was led by the Joint Research Center (JRC) with the objective of producing a global map of all burned areas in 2000 using data provided by the SPOT-VEGETATION 1-km spatial resolution sensor (Grégoire *et al.* 2003). The GLOBSCAR project, which is part of the European Space Agency (ESA) Data User Program, produced global incremental maps of burned areas on a monthly basis from the year 2000 using data gathered from the Along Track Scanning Radiometer (ATSR-2), an instrument fitted to the ESA ERS-2 satellite (Simon *et al.* 2004). The GLOBCARBON BAE Products are formed by combining the methods used in the GBA2000 and GLOBSCAR projects. These products detect the appearance of new burned areas from month to month and are available for the period 1998–2007. Finally, the MODIS Burned Area Product (MCD45A1: MODIS

 10.1071/WF07081 1049-8001/09/040404

Level 3 monthly tiled 500-m Burned Area Product), which is still in its provisional version, is expected to map fire-affected areas on a global scale using the MODIS surface reflectance time series (Roy *et al.* 2005). The algorithm developed by Roy *et al*. (2005), which is based on a bidirectional reflectance model-based expectation change detection approach, has proved able to perform consistently across different fire regimes. All the aforementioned datasets are available over the worldwide web free of charge.

Satellite-based strategies for burn mapping rely on two types of remote sensing data: post-fire images and active fires, both of which may be used separately or in combination. In the second method, fire thermal energy, as measured by mid-infrared channels, is used to identify active fires. This detection of active fires and the determination of their parameters have normally been carried out by polar orbiting sensors, like the Advanced Very High Resolution Radiometer – AVHRR (Kaufman *et al.* 1990; Justice *et al.* 1996; Giglio *et al.* 1999; Stroppiana *et al.* 2000), the Advanced Along-Track Scanning Radiometer – (A)ATSR (Kasischke *et al.* 2003) or MODIS (Justice *et al.* 2002; Giglio *et al.* 2003), and more recently, by sensors on board geostationary satellites like the Geostationary Operational Environmental Satellite – GOES (Prins and Menzel 1994) or the European Meteosat (Govaerts *et al.* 2002; Boschetti *et al.* 2003; Calle *et al.* 2006). However, the temporal and spatial patterns of biomass burning cannot be estimated reliably from active fire data, as the satellite may not pass over at the time of the fire, or the fire may be obscured owing to cloud cover or dense smoke (Roy *et al.* 2002). However, the use of active fire events could result in an overestimation of damaged area if the detection algorithms are not properly applied to the different environments (Fraser *et al.* 2000).

Owing to the aforementioned reasons, most of the burned area mapping has been done using post-fire satellite data, alone or in comparison with pre-fire information. This is based on the ability of remote sensing measurements to detect vegetation damage after fire, an effect that is temporally persistent in most ecosystems (Roy *et al.* 2002), including those of the Mediterranean. The range of methods dealing with scar mapping includes, among others (Koustias *et al.* 1999): (i) thresholding of single bands or indices (Hall *et al.* 1980); (ii) supervised and unsupervised classification of original bands or indices (Milne 1986); (iii) multivariate analysis of original bands (Tanaka *et al.* 1983); (iv) spectral mixture analysis (Cochrane and Souza 1998; González-Alonso *et al.* 2007); (v) time-series analysis (Milne 1986; Roy *et al.* 2002, 2005). This array of methods has succeeded in producing highly valuable results in different ecosystems and with different datasets. However, most methodologies are not usually readily adaptable to every dataset used, particularly those relying on fixed thresholds whose definition is 'problematic due to variations in both the surface state and those imposed by the sensing system' (Roy *et al.* 2002). Although different approaches have been proposed to reduce threshold sensitivity to the different factors involved (Fraser *et al.* 2000; Roy *et al.* 2002), most methods still fail to account for certain variations such as those derived from the sun–target–sensor geometries (McDonald *et al.* 1998).

Among the different methods for burn mapping by means of post-fire satellite data, the use of spectral indices is one of the most widespread. Vegetation indices (e.g. NDVI – Normalised Difference Vegetation Index), whose estimation typically involves data from the red and near-infrared (NIR) bands, have been commonly used to derive vegetation properties but also to discriminate and map burned areas (Pereira *et al.* 1999). However, these indices 'were not designed for discrimination of burned surfaces, and therefore they may not be well adapted to differentiate carbon-charcoal, which is the predominant material derived in recently fire-affected areas' (Martín *et al.* 2006). According to Lentile *et al*. (2006), in most environments and fire regimes and at the spatial resolution of most satellite sensors (pixel size >30 m), burned vegetation results in a drastic reduction in NIR surface reflectance, which is typically accompanied by a rise in shortwave infrared (SWIR) reflectance. As stated by Pereira *et al*. (1997; cited in Roy *et al.* 2002), the use of NIR and SWIR to obtain burn mapping results is more appropriate because these two bands have been found to provide stronger burned area discrimination than visible wavelengths. In this way, the Normalised Burn Ratio (NBR) and the differenced NBR (dNBR) indices integrate the NIR and SWIR bands, both of which register the strongest response, albeit in opposite ways, to burning (Key 1999; Roldán-Zamarrón *et al.* 2006).

Another set of spectral indices for burn discrimination are those based 'on maximising the spectral distance between coal/charcoal and other land covers, especially those potentially confused with burned areas' (Martín *et al.* 2005, 2006). Based on these ideas, the Burned Area Index (BAI) was originally defined in the red and NIR spectral domain, when it was used to discriminate recently burned areas in NOAA-AVHRR (National Oceanic and Atmospheric Administration–Advanced Very High Resolution Radiometer) images (Chuvieco *et al.* 2002). This index is estimated using the following equation:

$$\mathrm{BAI} = 1/((\rho c_r - \rho_r)^2 + (\rho c_{nir} - \rho_{nir})^2) \quad (1)$$

where ρc_r and ρc_{nir} are the red and NIR reference reflectance values, respectively, and ρ_r and ρ_{nir} are the pixel reflectances in the same bands. The MODIS Burned Area Index (BAIM) is a new version of the BAI adapted to the spectral resolution of MODIS reflective bands for mapping recently burned areas in Mediterranean ecosystems. The utility of the BAIM to map burned areas was assessed against other spectral indices (Mid-Infrared Burn Index – MIRBI, BAI and NBR) using MODIS data over the Iberian Peninsula and it provided the greatest discrimination ability (Martín *et al.* 2005, 2006). The BAIM is estimated using the following equation:

$$\mathrm{BAIM} = 1/((\rho c_{nir} - \rho_{nir})^2 + (\rho c_{swir} - \rho_{swir})^2) \quad (2)$$

where ρc_{nir} and ρc_{swir} are the NIR and SWIR reference reflectance values, respectively, and ρ_{nir} and ρ_{swir} are the pixel reflectances in the same bands.

Another approach to be considered for burn mapping is the integration of spectral indices and active fire information. Following this model, Roy *et al*. (1999) developed a multitemporal burn scar detection algorithm that used a time series of burn scar index data (based on a vegetation index), as derived from AVHRR daily images, to compute a burn scar index change map that was then classified using thresholds derived from the output of an active fire detection algorithm. Fraser *et al*. (2000) also

used AVHRR data to develop their hotspot and NDVI differencing synergy (HANDS) algorithm, an approach that combines the strengths of hotspot detection and NDVI differencing for boreal burned area mapping. Al-Rawi *et al*. (2001) tried to go beyond designing a system for monitoring the status of a fire in real time by creating a system that would also produce a near-real time burned area map. To do so, Al-Rawi *et al*. (2001) used NDVI–Maximum Value Composites as well as active fire locations, both derived from AVHRR data. Another approach is that taken by Pu *et al*. (2004) who proposed an algorithm based on fire dynamics on a daily basis to obtain daily information on active fires and burn scars, using AVHRR data from California for NDVI calculation and hotspot detection.

The work presented here assesses the estimation and mapping of burned areas in Galicia (north-west Spain) in 2006 using a method that also integrates spectral indices with active fire data. However, in this case, burn mapping is based on just one post-fire high spatial resolution image (from Resourcesat-1: AWiFS – Advanced Wide Field Sensor), which reduces time for data preprocessing and enhances the scale of the final product. This method uses a burn area spectral index (based on the BAIM) instead of vegetation indices, which are supposed to be less sensitive to the changes in the spectral properties of a land surface after fire. In addition, the use of active fire data (as derived from Terra/Aqua–MODIS) is original in the way it is applied to both index threshold determination and commission errors removal, as explained in a later section.

Study area and dataset description

The approach is applied here to Galicia (Spain) where hundreds of forest fires occurred during the first 20 days of August 2006. This region, situated in the north-west of the Iberian Peninsula, just to the north of Portugal, is one of the most humid parts of Spain. The study area covers 29 681.65 km^2, almost 70% of which, according to the Third National Forest Inventory (1997–2006, Ministerio de Medio Ambiente 2005), is classified as 'forested', with 64% being tree-covered (conifers and eucalyptus mainly). In this region, woodland fires are usually small but frequent. In fact, Galicia is undoubtedly the region with the greatest concentration of wildfires in Spain. During August 2006, nearly 930 km^2 were almost entirely burned over the course of 8 days, producing significant economic losses and severe social upheaval. It is thought that ~90% of the forest fires were caused by people.

Three types of data were used for the current work: (i) a post-fire satellite image; (ii) active fire data; and (iii) ancillary maps and information. We used a post-fire image from the AWiFS sensor onboard the Indian satellite Resourcesat-1, dated 21 August 2006, as well as MODIS active fire data for the first 20 days of August 2006 (see Fig. 1). AWiFS is a unique sensor, providing data with a spatial resolution of 56 m at 5-day intervals (Seshadri *et al.* 2005) in four spectral bands (green, red, NIR and SWIR; see Table 1). MODIS is a sensor housed on Terra and Aqua NASA (National Aeronautics and Space Administration) satellites with more than 30 channels at variable spatial resolutions (250 to 1000 m), two of which are thermal bands (1000-m pixel size) used for active fire detection. A general description of the MODIS fire products can be found in Justice *et al*. (2002). A detailed description of the MODIS active fire detection algorithm (version 4) can be found in Giglio *et al*. (2003). The ancillary maps and information we used consisted of: (i) a digital terrain model for AWiFS image preprocessing, and (ii) the CORINE (Coordinate Information on the Environment) Land Cover 2000 coverage (CLC2000, European Environment Agency, see http://dataservice.eea.eu.int, accessed June 2007) for masking purposes.

The MODIS Hotspot–Active Fire Detections (NASA and University of Maryland 2002), as provided free of charge through the Internet, consist of a set of shape files (one per year) with one record per active fire. Information related to each active fire included: location (latitude and longitude), date, time, confidence level and satellite involved (Terra or Aqua). The particular area in question, Galicia (~30 000 km^2) experienced 3340 active fires in the first 20 days of August 2006.

Methodology

All burned area estimation and mapping followed four steps: (i) BAIM calculation using the AWiFS image; (ii) BAIM threshold establishment; (iii) CLC2000 mask application; and (iv) active fire analysis for final burned area map production. The BAIM was calculated using satellite reflectances; thus, the AWiFS image needed to be preprocessed as explained in the next section. Image and data processing was carried out using *ENVI 4.2* (ITT Corp., Boulder, CO) and *ArcView 3.2* (ESRI, Redlands, CA) software packages.

AWiFS image preprocessing

Prior to BAIM estimation, the AWiFS image was preprocessed. This involved radiometric and geometric corrections as the image was provided in raw format (digital numbers not geometrically corrected). The radiometric correction consisted of two stages: (i) sensor calibration (conversion of digital numbers into radiance values); and (ii) reflectance estimation (conversion of radiance values into reflectance values). The sensor calibration was carried out using pre-launch laboratory values of gain and bias. The various parameters needed for estimating spectral reflectance are: maximum and minimum radiances in the satellite sensor bands, mean solar exo-atmospheric irradiances, image acquisition time, solar declination, solar angles (zenith and azimuth) and mean Earth–Sun distance. At that time, no atmospheric correction was performed given that no atmospheric or meteorological data were available for the time of image acquisition. Fortunately, the bands used for BAIM estimation are the least affected by atmospheric scattering.

The resulting 'top-of-atmosphere' reflectance image was orthorectified using a digital elevation model (25-m spatial resolution) for correction of terrain effect, and the corresponding 'geometrical calibration files' (also known as 'RPC' files) for internal calibration. Geometric accuracy was tested using digital maps showing coastline and water bodies.

Burned area mapping

As mentioned previously, the BAIM estimation was the first step in the projected burned area mapping. The BAIM was specifically defined to discriminate between burned and unburned areas

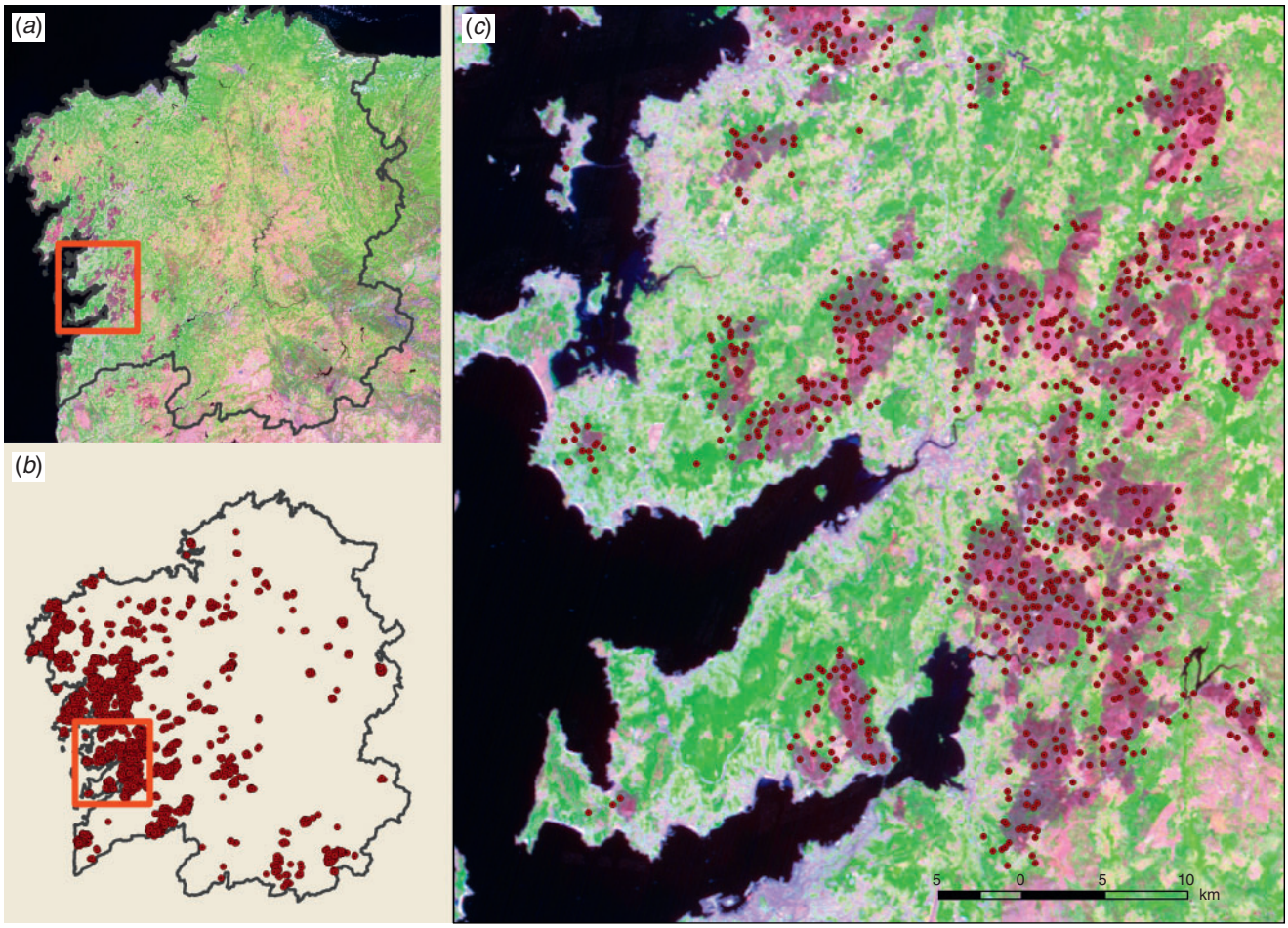

Fig. 1. AWiFS (Advanced Wide Field Sensor) post-fire image (dated 21 August 2006, red–green–blue composition: 543) (*a*); MODIS (Moderate Resolution Imaging Spectrometer) active fires (dated 1 to 20 August 2006) (*b*); and most burned areas (darker) presented MODIS active fires (*c*).

Table 1. AWiFS (Advanced Wide Field Sensor) sensor characteristics (NIR: near-infrared; SWIR: shortwave infrared)

	B2 (green)	B3 (red)	B4 (NIR)	B5 (SWIR)
Spatial resolution (m)	56	56	56	56
Swath width (km)	740	740	740	740
Temporal resolution (days)	2–5	2–5	2–5	2–5
Spectral resolution (μm)	0.52–0.59	0.62–0.68	0.77–0.86	1.55–1.70

using data from the Terra&Aqua MODIS sensor (Martín *et al.* 2006). It is based on its predecessor, the BAI, which is 'computed from the spectral distance from each pixel to a reference spectral point, where recently burned areas tend to converge' (Chuvieco *et al.* 2002). The BAIM uses 'concentric distances to a convergence point, defined from radiative properties of recently burned areas in the NIR and SWIR bands' (Martín *et al.* 2006). It is calculated using pixel reflectance values in the NIR (MODIS band 2 at 0.841–0.876 μm) and SWIR (MODIS band 7 at 2.105–2.155 μm) bands as well as using NIR and SWIR reference reflectance values, those corresponding to the aforementioned convergence point. Such reference values are usually calculated based on the literature available and the analysis of several sets of satellite sensor images (Chuvieco *et al.* 2002).

For the present work, reference reflectance values were calculated using the AWiFS image itself, given the absence of existing published values. To do so, we used the statistical distribution of burned pixel reflectances, as extracted from the relevant bands (band 4 in the NIR and band 5 in the SWIR, see Table 1), by means of manual digitalisation of more than 150 training areas. The digitalisation process was carried out by an expert throughout the study area using both the original bands (displayed using

Table 2. Reflectance values: summary statistics for a subset of burned pixels in the NIR (near-infrared) and SWIR (shortwave infrared) bands of the AWiFS (Advanced Wide Field Sensor) image

	Count	Minimum	Maximum	Mean	Standard deviation
AWiFS B4 (NIR)	6611	0.0517	0.1509	0.0845	0.0146
AWiFS B5 (SWIR)	6611	0.0821	0.2300	0.1438	0.0257

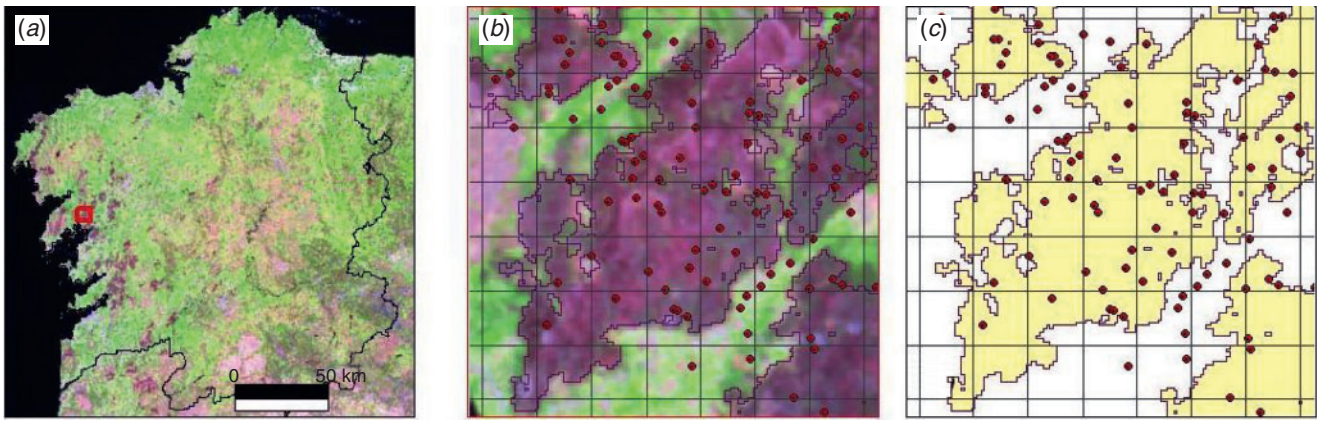

Fig. 2. AWiFS (Advanced Wide Field Sensor) post-fire image (dated 21 August 2006, red–green–blue composition: 543) (*a*); detail: correspondence between 'burned area' (delineated) and 'active fires' (dots), grid size of 1 km (*b*); and detail: correspondence between 'burned area' (delineated, shaded) and 'active fires', grid size of 1 km (*c*).

a red–green–blue composite) and some spectral indices (NDVI and NBR).

The reflectance information from the training areas, which accounted for 6611 AWiFS pixels, was analyzed first, in order to check the variability in the spectral signature of burned areas in the study area. Elementary statistics (see Table 2) showed little variability, thus permitting work to continue.

Van Wagtendonk *et al*. (2004) showed in their work on fire severity assessment using AVIRIS (Airborne Visible–Infrared Imaging Spectrometer) and Landsat ETM+ (Enhanced Thematic Mapper Plus) data that the higher the fire severity, the greater the negative response to fire in the NIR wavelengths and the greater the positive response to fire in the SWIR. Therefore, if we are looking for 'definitely burned' pixels within the AWiFS training areas because those pixels would give us the best definition of the BAIM, lower values are the most telling in the case of NIR bands, whereas the same is true of greater values in the case of SWIR bands. In this way, we would be maximising the distance between burned pixels and other potentially confusing land uses. In practice, we defined reference reflectance in the NIR (ρc_{nir}) as the 'ρ_{nir} value for 5% of accumulated probability (5th percentile, burned NIR reflectance distribution)' and reference reflectance in the SWIR (ρc_{swir}) as the 'ρ_{swir} value for 95% of accumulated probability (95th percentile, burned SWIR reflectance distribution)'. We used the 5 and 95% of accumulated probability instead of the minimum and maximum, respectively, in order to screen out any noise. The resulting reference reflectance values were 0.0561 and 0.1923 for the NIR and SWIR bands, respectively.

After the BAIM was calculated, a suitable threshold was established to distinguish between burned and unburned pixels. The BAIM threshold was determined based on the analysis of the best correlation between 'burned area' and 'number of accumulated MODIS active fires' for different grid sizes (1, 2, 3, 4, 5 km, etc.). An example is shown in Fig. 2. We started with the 1-km grid size, as this is the spatial resolution of the MODIS active fire product, and then kept on increasing grid size regularly up to 80 km (Galicia is covered by nine cells of 80 × 80 km). It was found that the coarser the spatial resolution of the grid, the better the correlation between 'burned area' and 'number of accumulated MODIS active fires' (results are only presented up to a 4-km grid size in Table 3). 'Burned area' was established retaining only those polygons containing at least one MODIS active fire inside. This technique may not identify all burns, but those identified are certain to be truly burned. BAIM threshold values originally considered for the analysis were: 80, 83, 85, 90, 95 and 100. Subsequently, the best correlation results, expressed in terms of the coefficient of determination, were found for a BAIM threshold value of 90 for all grid sizes (see Table 3). In the same table, an increase in the coefficient of determination as a function of grid size can be seen, which is due to the generalisation process caused by larger cell sizes and the resulting decrease in the sample size. The application of a threshold value of 90 resulted in a burned–unburned image that assured the greatest consistency between datasets concerning burned area (according to the BAIM criterion) and number of active forest fires as detected as thermal anomalies.

Table 3. Coefficients of determination between 'burned area' and 'number of active fires' for different BAIM (MODIS – Moderate Resolution Imaging Spectrometer – Burned Area Index) threshold values and grid sizes

BAIM	Grid sizes			
	1 × 1 km	2 × 2 km	3 × 3 km	4 × 4 km
80	41.16%	59.63%	66.62%	70.22%
83	43.38%	63.25%	71.04%	74.81%
85	44.85%	65.69%	74.02%	78.63%
90	45.80%	67.71%	76.58%	81.33%
95	45.07%	67.02%	76.18%	80.98%
100	44.29%	66.37%	75.24%	80.61%

In terms of spectral response in the optical range (visible and infrared), burns are very often confused with water bodies and other poorly reflective surfaces. Consequently, a vegetation mask was needed in order to screen out water bodies, urban or unvegetated areas and, in turn, produce a reliable burned area map. The selected forest mask was developed from the CLC2000 coverage, a European land cover database at a scale of 1 : 100 000. The CORINE Land Cover map comprises 85 different classes in the case of Spain; and 13 of those, classified as either 'unburnable' or 'non-forested', were found in the Galicia region. The mask obtained from this process was applied to a previous burned–unburned map, which produced improved results in terms of the map's accuracy. This map was subsequently converted into vector polygon format.

It is recognised that an effective threshold for separating burns is spatially variable (Fraser *et al.* 2000) because both the surface itself and the sensing system introduce variations in space (Roy *et al.* 2002). All the studies carried out on this subject have used one of the two possible approaches of fixed or variable thresholds. Many authors have favoured the use of the variable approach, but in the current study, we have opted for the fixed approach despite the problem of 'spatial variation'. We attempted to solve this through the use of the MODIS active fire data. The Galicia region is 30 000 km^2 in size, hosting a wide range of ecosystems from the Atlantic to the Mediterranean areas (west to east and north to south). Such spatial variation, combined with the threshold value we used, produced an excellent delineation of burned patches in the west part of Galicia, but a large number of commission errors in the south-east area in our study (see Fig. 3). As expected, the application of a fixed threshold did not result in burn mapping of homogeneous quality, no matter how precisely the BAIM threshold had been defined. Therefore, and to better cope with the diverse environments throughout Galicia, the burn mapping algorithm required a further step that consisted of using the MODIS active fire locations to confirm burned polygons, thus eliminating many 'false burns'. As shown in Fig. 1, most burned areas (which appear darker throughout the AWiFS image) revealed MODIS active fires inside; therefore, it was decided to use the latter to screen out clearly unburned polygons as well as small polygons (commission errors). The resulting map is shown in Fig. 4. Finally, a visual analysis of the image was carried out in order to recover some of the polygons that, being clearly affected by fire, had been eliminated for not containing active fires. The final burned area map appears in Fig. 5.

Results and discussion

Fig. 5 shows a burned area map for the Galicia region (north-west Spain) for the 2006 summer season until 21 August. The affected area was 932.61 km^2: more than 3% of total Galician territory. As explained in the methodology section, the first steps for burn mapping included BAIM estimation and threshold plus mask application, all of which resulted in a vector layer with 18 379 polygons that covered a total of 1730.49 km^2. Although this figure may appear elevated when compared with official statistics (burned area of 930 km^2), it was decided to keep the threshold value of 90, not only because it produced the best correlation (see Table 3) but also because it best delineated the boundaries of individual burns (especially in the west) in spite of producing many commission errors (thousands of small polygons) in the south-east. Greater BAIM threshold values would have generated a smaller number of commission errors but, however, they would also have produced smaller polygons that would have had to be corrected using complex techniques. Some authors propose dynamic thresholds based on the magnitude of one pixel relative to the surrounding pixels or to a time series (Fernández *et al.* 1997; Fraser *et al.* 2000; Roy *et al.* 2005). For the present work, however, it was decided to rely on the fixed threshold value that produced the best delineation and to screen out unburned polygons by using available information on active fires accumulated during the period of study. Active fires were thus used to maintain those polygons where fire had happened with a high degree of certainty, a process that produced 177 polygons, accounting for an area of 790.18 km^2.

As noted previously, active fire detection generally underestimates burned area owing to 'low satellite revisit frequency and obscuring by cloud and smoke' (Fraser *et al.* 2000) and a visual analysis of the 177-polygon layer (Fig. 4) confirms this point. Therefore, it was decided to manually recover those polygons that, appearing clearly affected by fire on the AWiFS image, did not contain at least one active fire inside. At this juncture, it has to be pointed out that although the focus was on the fire events of the first 20 days of August 2006, fire damage to vegetation remains evident for long periods, so we can confidently say that the AWiFS image analysed shows traces of previous wildfire events. Finally, a map with 317 polygons that covered 932.61 km^2 was produced, the last stage of manual recovery adding 140 polygons that accounted for 15% of the total damaged area only.

Although no thorough validation was carried out, the results from the present study were compared with the official fire statistics from both the Spanish Ministry of the Environment and the Galician Forestry Service. At that time it was not possible to validate results using perimeters from conventional mapping or field data. In spite of this, it was possible to carry out a visual analysis of the final map, resulting in a satisfactory and reliable product, thanks to the suitability of the spatial resolution of the AWiFS image for burn mapping on a regional scale. Moreover, the results tally with data from the Ministry of the Environment (Ministerio de Medio Ambiente 2006), which record figures of 929.41 km^2 of burned area for the Galicia region until 1 October 2006. Our analysis compared with the official record of burned

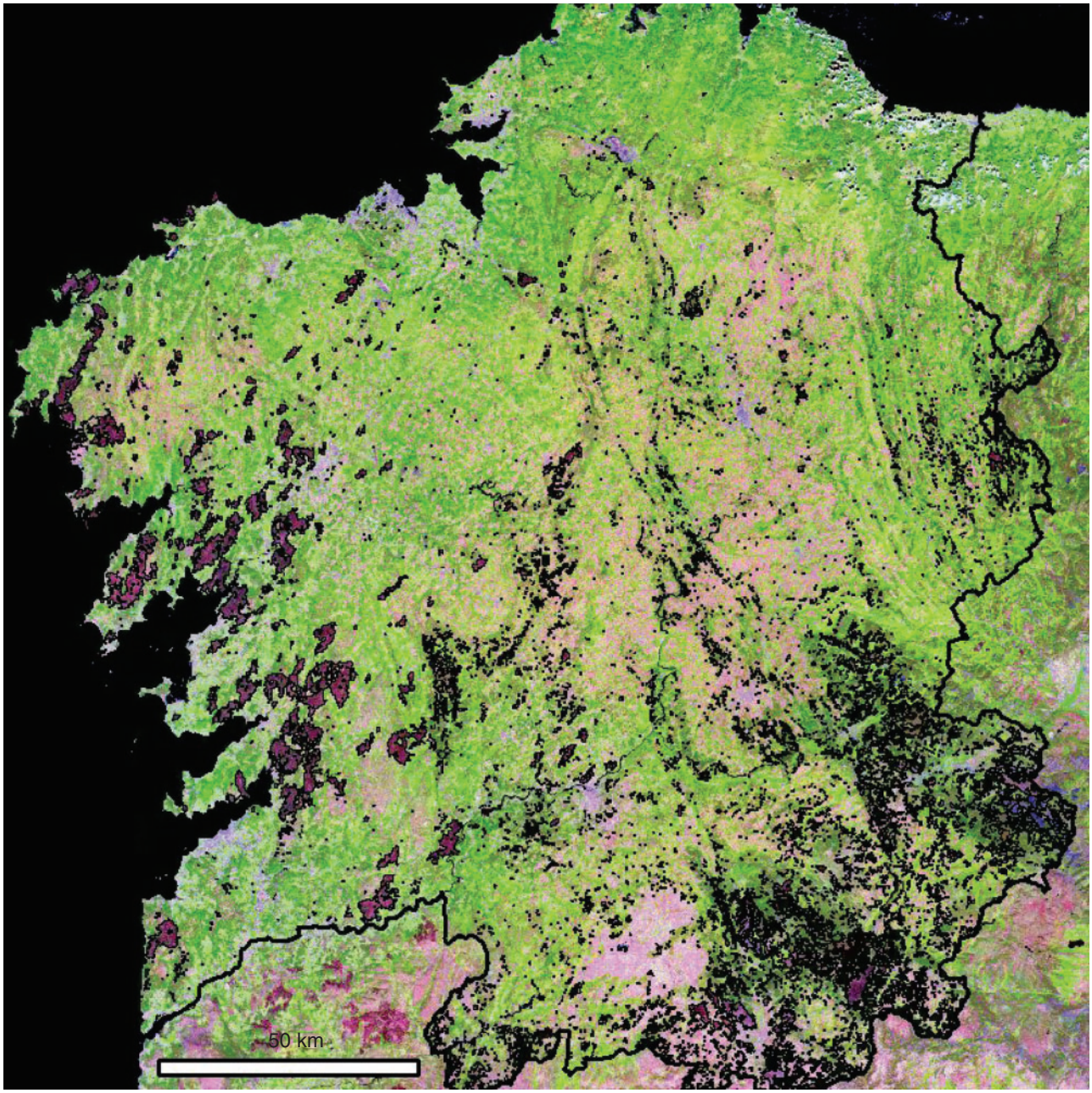

Fig. 3. Patches of BAIM (MODIS – Moderate Resolution Imaging Spectrometer – Burned Area Index) greater than 90 (vector format) over the AWiFS (Advanced Wide Field Sensor) image.

area per province is presented in Table 4, which shows that high-quality results were reached for three of the four provinces. The case of Lugo, where more than half the 'burned area' was missed, was analysed, concluding that either there had been a wildfire between 21 August (AWiFS image) and 1 October (Ministry of the Environment data) or there had been an early-season fire (or fires) after which the vegetation had partially recovered. According to the Galician authorities (Xunta de Galicia 2007), the affected area for the whole year was 938.87 km^2.

Conclusions

The present article presents a semiautomatic algorithm for burned area mapping using remote sensing techniques and data that was successfully applied to the Galicia region (Spain). It uses satellite information from four different parts of the spectrum (NIR, SWIR, middle- and thermal infrared, or MIR and TIR, respectively). We developed a methodology that is based on the combination of a spectral index with active fire locations, which builds on previous research (Roy *et al.* 1999; Fraser *et al.* 2000;

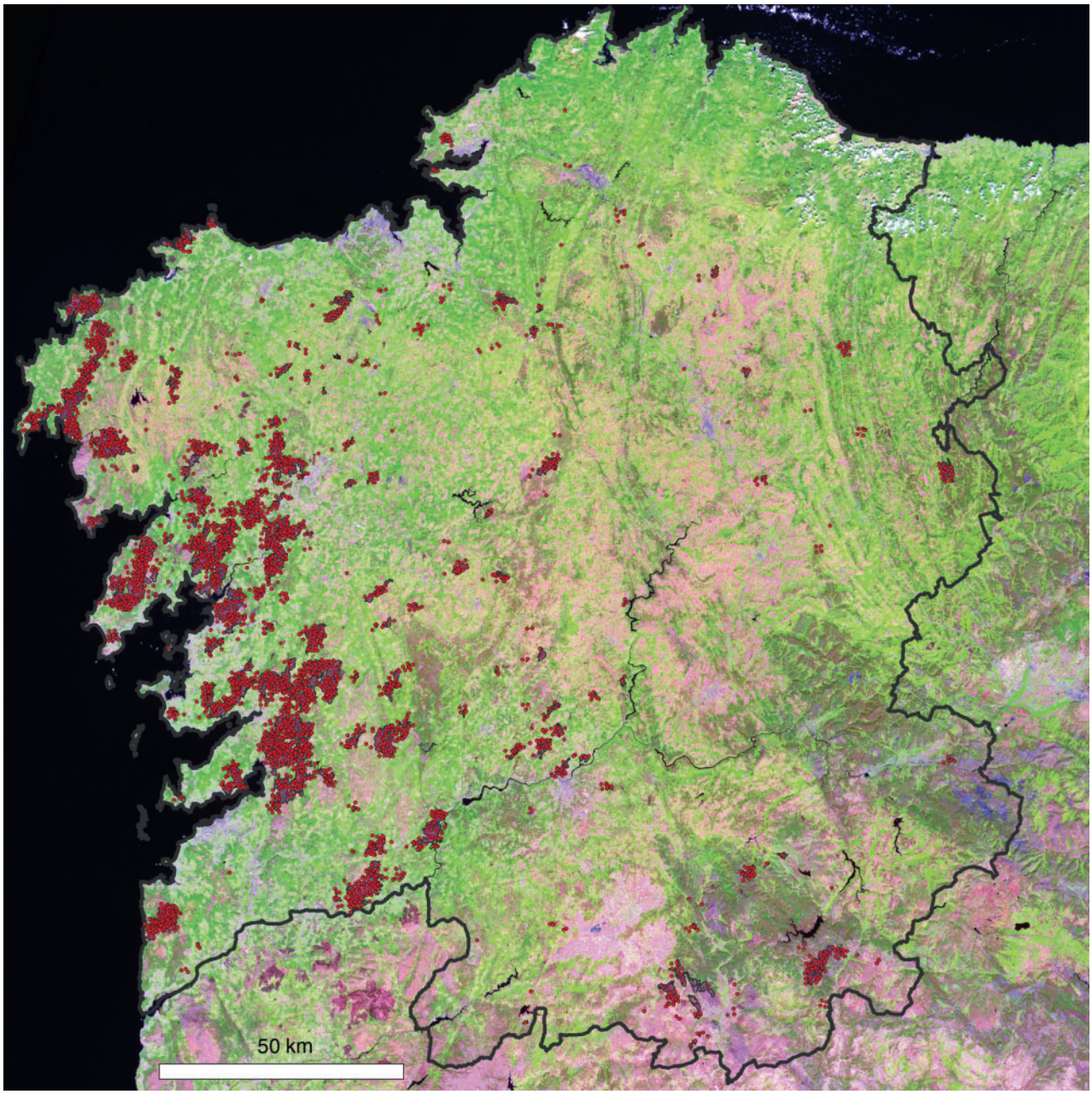

Fig. 4. Patches of BAIM (MODIS – Moderate Resolution Imaging Spectrometer – Burned Area Index) greater than 90 (vector format) and containing at least one active fire. Active fires are shown using a dot.

Al-Rawi *et al.* 2001; Pu *et al.* 2004) and also introduces innovations like the use of the BAIM (Martín *et al.* 2006) and AWiFS data. To be more precise, the BASA (Burned Area Synergic Algorithm) combines BAIM thresholding and active fire detection. BAIM (based on NIR and SWIR bands) thresholding is used to produce a 'burned–unburned' map while the active fire series (based on MIR and TIR bands) are used to remove falsely detected burns. The overall result is a close approximation to actual burn boundaries within the limits of the AWiFS pixel size. There are five advantages to the BASA method that are worth pointing out here: (i) preprocessing and processing of data is rapid; (ii) no field data are needed; (iii) not much human-based decision-making is required (objective method); (iv) it is easy to implement; and (v) it has been successfully applied at least once on a regional scale.

The methodology in question here has produced reliable results largely owing to its use of best correlation between two sets of data, each one coming from a different part of the spectrum. On the one hand, the BAIM is estimated using information from the NIR and SWIR channels, where reflective processes

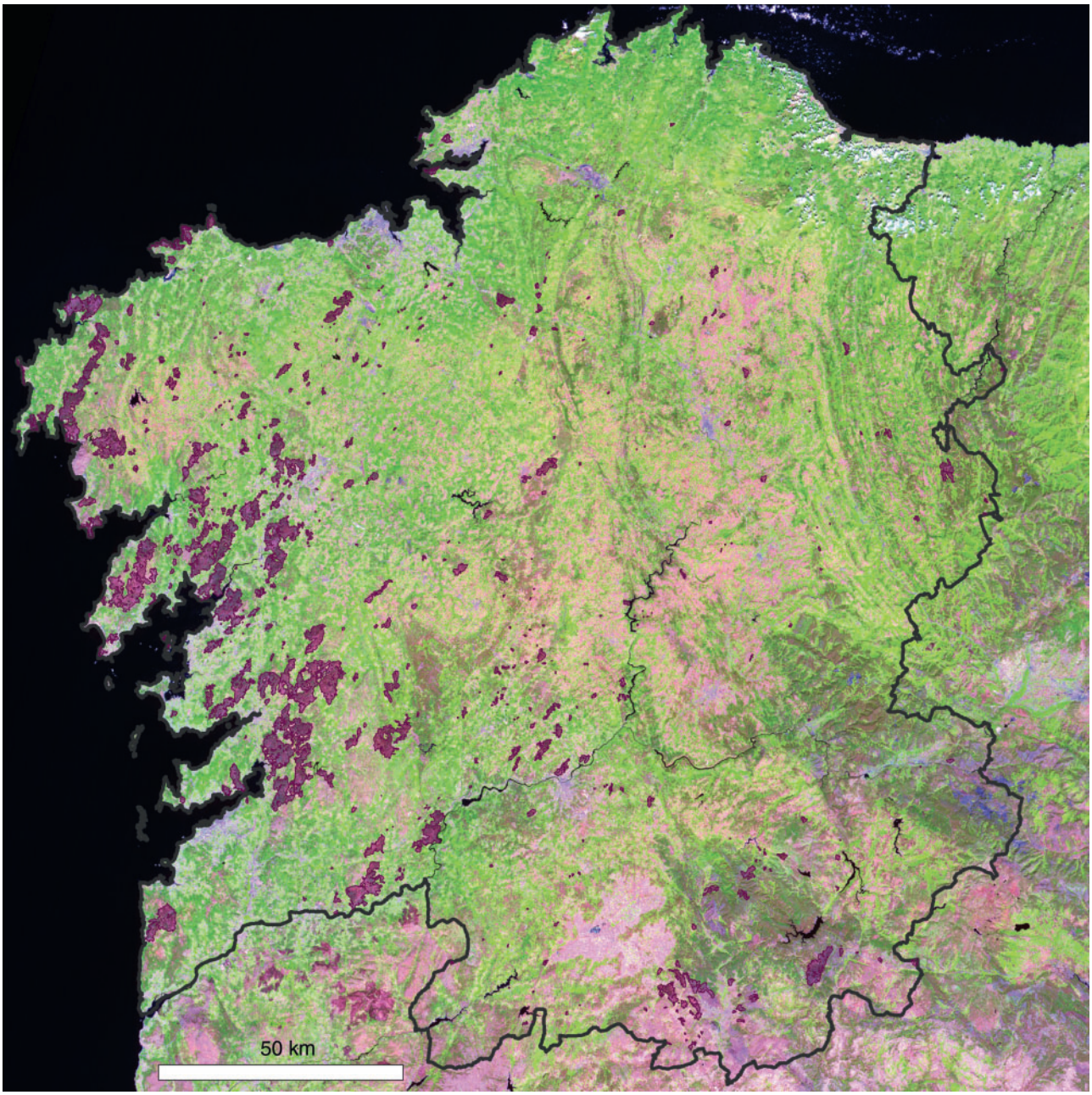

Fig. 5. Burned area map: patches of BAIM (MODIS – Moderate Resolution Imaging Spectrometer – Burned Area Index) greater than 90 and containing at least one active fire and manually recovered polygons.

are dominant. On the other, active fire data are elaborated using information from the emissive part of the spectrum, where the MIR and TIR channels are located. It is, however, important to note that as burn mapping results from the intersection of these two sets of data, the result will necessarily be adjusted to compensate for both commission and omission errors.

The use of AWiFS images for burned area mapping has proved to be very effective at a regional level owing to its combination of wide swath (740 km), high spatial resolution (56 m) and high temporal resolution (2–5 days). Owing to these characteristics, it is quite easy to find cloud-free scenes for burned area mapping over large regions, especially within the Mediterranean area.

Results obtained so far are quite satisfactory although further improvements will be studied in the future. One new development could consist of gradually improving the spatial resolution of satellite data, focussing on those areas where large numbers of forest fires concentrate. A suitable approach to this issue might begin with MODIS images, followed by AWiFS, Landsat-TM (Thematic Mapper), SPOT-HRG (Système pour l'Observation de la Terre–High Resolution Geometric instrument) and so on.

Table 4. Galicia burned area: figures from the Ministry of Environment *v.* results from the present study; areas expressed in km^2 per province; relative difference between both sets of data

	Ministry of Environment	Results from present study	Relative difference
A Coruña	345.04	366.26	6.15%
Lugo	60.80	27.02	−55.56%
Orense	120.67	123.49	2.34%
Pontevedra	402.90	415.84	3.21%
Galicia	929.41	932.61	0.34%

Acknowledgements

The authors would like to thank the Spanish National Geographic Institute (IGN) for helping us in the use of the CORINE Land Cover 2000 product and the NASA Land Processes Distributed Active Archive Center (LP DAAC) for supplying Terra/Aqua MODIS active fire products. The anonymous reviewers are also thanked for their comments.

References

Al-Rawi KR, Casanova JL, Romo A (2001) IFEMS: a new approach for monitoring wildfire evolution with NOAA-AVHRR imagery. *International Journal of Remote Sensing* **22**, 2033–2042. doi:10.1080/01431160152043694

Boschetti L, Brivio PA, Gregoire JM (2003) The use of Meteosat and GMS imagery to detect burned areas in tropical environments. *Remote Sensing of Environment* **85**, 78–91. doi:10.1016/S0034-4257(02)00189-X

Calle A, Casanova JL, Romo A (2006) Fire detection and monitoring using MSG Spinning Enhanced Visible and Infrared Imager (SEVIRI) data. *Journal of Geophysical Research* **111**, G04S06. doi:10.1029/2005JG000116

Chuvieco E (1999) Introduction. In 'Remote Sensing of Large Wildfires in the European Mediterranean Basin'. (Ed. E Chuvieco) pp. 1–3. (Springer: Berlin)

Chuvieco E, Martín MP, Palacios A (2002) Assessment of different spectral indices in the red–near-infrared spectral domain for burned land discrimination. *International Journal of Remote Sensing* **23**, 5103–5110. doi:10.1080/01431160210153129

Cochrane MA, Souza CM (1998) Linear mixture model classification of burned forests in the Eastern Amazon. *International Journal of Remote Sensing* **19**, 3433–3440. doi:10.1080/014311698214109

Crutzen PJ, Andreae MO (1990) Biomass burning in the Tropics: impact on atmospheric chemistry and biogeochemical cycles. *Science* **250**, 1669–1678. doi:10.1126/SCIENCE.250.4988.1669

Fernández A, Illera P, Casanova JL (1997) Automatic mapping of surfaces affected by forest fires in Spain using AVHRR NDVI composite image data. *Remote Sensing of Environment* **60**, 153–162. doi:10.1016/S0034-4257(96)00178-2

Fraser RH, Li Z, Cihlar J (2000) Hotspot and NDVI Differencing Synergy (HANDS): a new technique of burned area mapping over boreal forest. *Remote Sensing of Environment* **74**, 362–376. doi:10.1016/S0034-4257(00)00078-X

Giglio L, Kendall JD, Justice CO (1999) Evaluation of global fire detection algorithms using simulated AVHRR infrared data. *International Journal of Remote Sensing* **20**, 1947–1985. doi:10.1080/014311699212290

Giglio L, Descloitres J, Justice CO, Kaufman YJ (2003) An enhanced contextual fire detection algorithm for MODIS. *Remote Sensing of Environment* **87**, 273–282. doi:10.1016/S0034-4257(03)00184-6

González-Alonso F, Merino-de-Miguel S, Roldán-Zamarrón A, García-Gigorro S, Cuevas JM (2007) MERIS Full Resolution data for mapping level-of-damage by forest fires: the Valencia de Alcántara event in August 2003. *International Journal of Remote Sensing* **28**, 797–809. doi:10.1080/01431160600979115

Govaerts YM, Pereira JM, Pinty B, Mota B (2002) Impact of fires on surface albedo dynamics over the African continent. *Journal of Geophysical Research* **107**(D22), 4629. doi:10.1029/2002JD002388

Grégoire JM, Tansey K, Silva JMN (2003) The GBA initiative: developing a global burned area database from SPOT-VEGETATION imagery. *International Journal of Remote Sensing* **24**, 1369–1376. doi:10.1080/0143116021000044850

Hall DK, Ormsby JP, Honhson L, Brown J (1980) Landsat digital analysis of the initial recovery of burned tundra at Kokolik River, Alaska. *Remote Sensing of Environment* **10**, 263–272. doi:10.1016/0034-4257(80)90086-3

Houghton JT, Meira Filho LG, Bruce J, Lee H, Callander BA, Haites E, Harris N, Maskell K (1995) 'Climate Change 1994: Radiative Forcing of Climate Change.' (Cambridge University Press: Cambridge, UK)

Justice CO, Kendall JD, Dowty PR, Scholes RJ (1996) Satellite remote sensing of fires during the SAFARI campaign using NOAA Advanced Very High Resolution Radiometer data. *Journal of Geophysical Research* **101**, 23 851–23 863. doi:10.1029/95JD00623

Justice CO, Giglio L, Korontzi S, Owens J, Morisette JT, Roy DP, Descloitres J, Alleaume S, Petitcolin F, Kaufman Y (2002) The MODIS fire products. *Remote Sensing of Environment* **83**, 244–262. doi:10.1016/S0034-4257(02)00076-7

Kasischke ES, Hewson JH, Stocks B, van der Werf G, Randerson J (2003) The use of ATSR active fire counts for estimating relative patterns of biomass burning – a study from the boreal forest region. *Geophysical Research Letters* **30**(18), 1969. doi:10.1029/2003GL017859

Kaufman Y, Tucker C, Fung I (1990) Remote sensing of biomass burning in the tropics. *Journal of Geophysical Research* **95**, 9927–9939. doi:10.1029/JD095ID07P09927

Key CH (1999) The Normalized Burn Ratio (NBR): a Landsat TM Radiometric measure of burn severity. United States Geological Survey, Northern Rocky Mountain Science Center. (Bozeman, MT)

Koustias N, Karteris M, Fernández-Palacios A, Navarro C, Jurado J, Navarro R, Lobo A (1999) Burnt land mapping at local scale. In 'Remote Sensing of Large Wildfires in the European Mediterranean Basin'. (Ed. E Chuvieco) pp. 157–187. (Springer: Berlin)

Lentile LB, Holden ZA, Smith AMS, Falkowski MJ, Hudak AT, Morgan P, Lewis SA, Gessler PE, Benson NC (2006) Remote sensing techniques to assess active fire characteristics and post-fire effects. *International Journal of Wildland Fire* **15**, 319–345. doi:10.1071/WF05097

Martín MP, Gómez I, Chuvieco E (2005) Performance of a burned-area index (BAIM) for mapping Mediterranean burned scars from MODIS data. In 'Proceedings of the 5th International Workshop on Remote Sensing and GIS applications to Forest Fire Management: Fire Effects Assessment', 16–18 June 2005, Zaragoza, Spain. (Eds J de la Riva, F Pérez-Cabello, E Chuvieco) pp. 193–197. (Universidad de Zaragoza: Zaragoza)

Martín MP, Gómez I, Chuvieco E (2006) Burnt Area Index (BAIM) for burned area discrimination at regional scale using MODIS data. *Forest Ecology and Management* **234**(Suppl.), S221. doi:10.1016/J.FORECO.2006.08.248

McDonald AJ, Gemmell FM, Lewis PE (1998) Investigation of the utility of spectral vegetation indices for determining information on coniferous forests. *Remote Sensing of Environment* **66**, 250–272. doi:10.1016/S0034-4257(98)00057-1

Milne AK (1986) The use of remote sensing in mapping and monitoring vegetation change associated with bushfire events in Eastern Australia. *Geocarto International* **1**, 25–32. doi:10.1080/10106048609354022

Ministerio de Medio Ambiente (2005) 'Tercer Inventario Forestal Nacional.' (Ministerio de Medio Ambiente: Madrid, Spain)

Ministerio de Medio Ambiente (2006) Incendios forestales en España 2006. Avance Informativo. (Ministerio de Medio Ambiente y Medio Rural y Marino: Madrid, Spain) Available at http://www.mma.es/portal/secciones/biodiversidad/defensa_incendios/ [Verified 18 March 2009]

Mitri GH, Gitas IZ (2006) Fire type mapping using object-based classification of Ikonos imagery. *International Journal of Wildland Fire* **15**, 457–462. doi:10.1071/WF05085

NASA, University of Maryland (2002) MODIS Hotspot/Active Fire Detections. Data set. MODIS Rapid Response Project. (University of Maryland: College Park, MD) Available at http://maps.geog.umd.edu [Verified 18 March 2009]

Pereira JMC, Chuvieco E, Beaudoin A, Desbois N (1997). Remote sensing of burned areas: a review. In 'A Review of Remote Sensing Methods for the Study of Large Wildland Fires'. (Ed. E Chuvieco) pp. 127–184. (Universidad de Alcalá: Alcalá de Henares)

Pereira JMC, Sa ACL, Sousa AMO, Martín MP, Chuvieco E (1999) Regional-scale burnt area mapping in Southern Europe using NOAA-AVHRR 1-km data. In 'Remote Sensing of Large Wildfires in the European Mediterranean Basin'. (Ed. E Chuvieco) pp. 139–155. (Springer: Berlin)

Prins EM, Menzel WP (1994) Trends in South American burning detected with the GOES VAS from 1983–1991. *Journal of Geophysical Research* **99**(D8), 16 719–16 735. doi:10.1029/94JD01208

Pu R, Gong P, Li Z, Scarborough J (2004) A dynamic algorithm for wildfire mapping with NOAA/AVHRR data. *International Journal of Wildland Fire* **13**, 275–285. doi:10.1071/WF03054

Roldán-Zamarrón A, Merino-de-Miguel S, González-Alonso F, García-Gigorro S, Cuevas JM (2006) Minas de Riotinto (South Spain) forest fire: burned area assessment and fire severity mapping using Landsat 5-TM, Envisat-MERIS and Terra-MODIS post-fire images. *Journal of Geophysical Research* **111**, G04S11. doi:10.1029/2005JG000136

Roy DP, Giglio L, Kendall JD, Justice CO (1999) Multi-temporal active-fire based burn scar detection algorithm. *International Journal of Remote Sensing* **20**, 1031–1038. doi:10.1080/014311699213073

Roy DP, Lewis PE, Justice CO (2002) Burned area mapping using multi-temporal moderate spatial resolution data – a bi-directional reflectance model-based expectation approach. *Remote Sensing of Environment* **83**, 263–286. doi:10.1016/S0034-4257(02)00077-9

Roy DP, Jin Y, Lewis PE, Justice CO (2005) Prototyping a global algorithm for systematic fire-affected area mapping using MODIS time series data. *Remote Sensing of Environment* **97**, 137–162. doi:10.1016/J.RSE.2005.04.007

Seshadri KSV, Rao M, Jayaraman V, Thyagarajan K, Murthi KRS (2005) Resourcesat-1: a global multi-observation mission for resources monitoring. *Acta Astronautica* **57**, 534–539. doi:10.1016/J.ACTAASTRO.2005.03.050

Simon M, Plummer S, Fierens F, Holzmann JJ, Arino O (2004) Burnt area detection at global scale using ATSR-2: the GLOBSCAR products and their qualification. *Journal of Geophysical Research* **109**, D14S02. doi:10.1029/2003JD003622

Stroppiana D, Pinnock S, Grégoire JM (2000) The global fire product: daily occurrence from April 1992 to December 1993 derived from NOAA AVHRR data. *International Journal of Remote Sensing* **21**, 1279–1288. doi:10.1080/014311600210173

Tanaka S, Kimura H, Suga Y (1983) Preparation of a 1 : 25000 Landsat map for assessment of burnt area on Etajima Island. *International Journal of Remote Sensing* **4**, 17–31. doi:10.1080/01431168308948528

Van der Werf GR, Randerson JT, Giglio L, Collatz GJ, Kasibhatla PS, Arellano AF (2006) Interannual variability in global biomass burning emissions from 1997 to 2004. *Atmospheric Chemistry and Physics* **6**, 3423–3441.

Van Wagtendonk JW, Root RR, Key CH (2004) Comparison of AVIRI and Landsat ETM+ detection capabilities for burn severity. *Remote Sensing of Environment* **92**(3), 397–408. doi:10.1016/J.RSE.2003.12.015

Xunta de Galicia (2007) Superficies quemadas en 2006. (Xunta de Galicia: Galicia, Spain) http://mediorural.xunta.es/ [Verified 18 March 2009]

Manuscript received 18 June 2007, accepted 21 May 2008